New method for modelling and design of multiconductor airborne antennas

G. Marrocco and P. Tognolatti

Abstract: A new approach is proposed, based on numerical (FDTD) and analytical (multiconductor transmission line MTL) tools, for the modelling of HF loop antennas mounted on aircraft. This method can be used to calculate the significant mutual coupling and the interaction with the body of the aircraft and also to perform fast optimisation of antenna size and position.

1 Introduction

In many application areas, such as HF airborne communications and planar technology transmitters, multiconductor transmission lines (MTL) are often used as radiating elements. Sometimes a number of straight conductors, placed at a small mutual distance, are connected to a larger body which presents a locally cylindrical region, at least in the close surroundings of the antennas. An example is the HF transmitting system (voice and data) of modern aeroplanes and helicopters for beyond-line-of-sight communication [1]. In this case, two parallel rectangular loop antennas (also known as 'towel bar' antennas) are mounted on the aircraft fuselage. Another example is a planar quasioptical frequency multiplier [2], where doubly folded dipoles are connected to the rest of the antenna.

With reference to the airborne system, the cylindrical body of the aircraft becomes an active part of the antenna, especially at lower frequency of the HF band, since it strongly interacts with the antennas and modifies their input impedance and radiation pattern. Antenna design and installation therefore require the cylindrical body to be carefully taken into account.

Although fullwave numerical simulations of the whole structure can nowadays be performed by numerical solvers running on high-speed computers, analytical or semianalytical models are still attractive for the purpose of model validation, and in particular for fast parametric analysis of antenna coupling and interaction with the surrounding environment. Simplified configurations, such as single antenna [3] or twin antennas [4] over perfect ground, have been solved by closed forms. The coupling between two parallel towel-bar antennas mounted on a cylindrical body has been analysed in [1] by means of a lumped-element equivalent circuit to corroborate numerical models and measurements at the lower bound of the HF band. The effect of the cylindrical body has been modelled by a lumped impedance, derived by an approximated closed form, which accounts for current flowing longitudinally on the airframe. However, this circuit is limited to frequencies for which the longitudinal length of the cylinder does not exceed one half wavelength, i.e. below the first fuselage resonance.

This paper proposes a novel approach to the analysis of this class of radiating multiconductor structures involving antennas of equal lengths, which still preserves the accuracy of fullwave modelling and permits a huge saving in computational needs. This approach, for which the preliminary idea was presented by the authors in [5], is based on a combined model, partly numerical, concerning the application of the finite difference time-domain (FDTD) method [6] to the analysis of the aircraft fuselage, and partly analytical for the loop model. A generalisation of the Γ/T-match feeding technique for dipole antennas [7, 8] is employed. With reference to the aircraft example, the three-conductor transmission line, originated by the fuselage and the two loops, is then analysed by the superposition of an antenna mode and two transmission line modes. Line parameters are calculated by solving an integral equation for static charge distribution on a two-dimensional structure. An equivalent circuit, incorporating transmission line sections, can therefore be derived, and the influence of the aircraft body is taken into account by global electrical information obtained from a coarse-grid FDTD solution of the aircraft without loops.

The model permits almost instantaneous wideband predictions of antenna coupling much beyond the first resonance of the main body and allows parametric analysis of the antenna system, as well as optimisation of geometrical parameters, to be carried out without repetition of time-consuming numerical runs.

2 Problem formulation

A first simplified formulation is described with reference to Fig. 1*a*. Two equal-size half-rectangular loops with length ℓ and height $s \ll \lambda$ are mounted on a larger cylindrical body of radius R and length L at the same longitudinal position z_g. The loops are spaced by an angle ϕ_0 and they lie on two planes sharing the cylinder axis. The system therefore possesses a longitudinal symmetry plane. The purpose of the following formulation is the computation of the input impedance or admittance matrix of this structure, without performing a fullwave analysis of the whole geometry.

The structure can be considered as a thick dipole (the cylindrical body) fed by two thin-conductor stubs. This arrangement is a two-port version (Fig. 1*b*) of the Γ-match

IEE Proceedings online no. 20040178

doi:10.1049/ip-map:20040178

Paper first received 1st April and in revised form 15th October 2003

G. Marrocco is with the DISP Università di Tor Vergata, Via del Politecnico 1, Roma 1-67040, Italy

P. Tognolatti is with the DIEL Università de L'Aquila, Monteluco di Roio, L'Aquila 1-67040, Italy

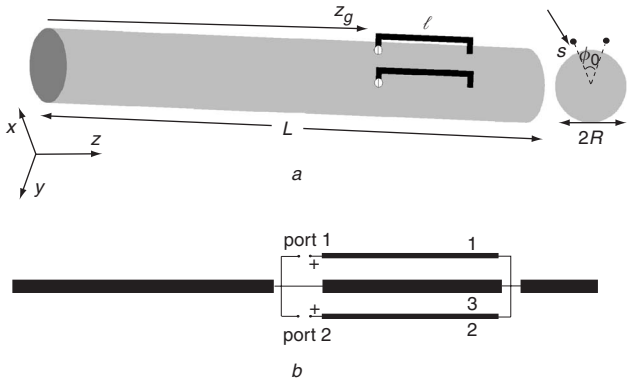

Fig. 1 *Multiconductor antenna model*
a Geometry of the structure under study, small circles indicating input ports
b Generalised *Γ-match* feeding model

configuration which is commonly used to match a coaxial transmission line to a dipole antenna. As a generalisation of the model proposed in [7, 8], our geometry will be studied as superposition of an antenna mode and two transmission line modes for the three-conductor line in the region of the loops, conductors 1 and 2 being the loops and conductor 3 the cylinder. The couplets $(V_i I_i)$, $i = 1 \ldots 3$, denote the voltages and currents at the three ports of the circuit depicted in Fig. 1*b*, (V_3, I_3 referring to an auxiliary port in the thicker cylinder, short-circuited in the Figure).

2.1 Lossless case

For the sake of simplicity, the case of lossless conductors is considered first. The influence of real conductors will be considered afterwards as a refinement of the model.

The currents I_1, I_2 and I_3 on the conductors are decomposed into an antenna mode (I_A) and two transmission line mode currents (even I_{Te} and odd I_{To})

$$\begin{bmatrix} I_1 \\ I_2 \\ I_3 \end{bmatrix} = \begin{bmatrix} \frac{1}{2+\alpha} & 1 & 1 \\ \frac{1}{2+\alpha} & 1 & -1 \\ \frac{\alpha}{2+\alpha} & -2 & 0 \end{bmatrix} \cdot \begin{bmatrix} I_A \\ I_{Te} \\ I_{To} \end{bmatrix} \tag{1}$$

Here α is a 'current (or charge) division factor', defined when all conductors are at the same potential V_0, which depends on the conductor cross-section boundaries C_i. This factor can be computed as $\alpha = Q_3/Q_2 = Q_3/Q_1$, where $Q_i = \int_{C_i} q_i(\mathbf{r}')dl'$, and the charge densities q_i are solutions of the following integral equation [9]:

$$\frac{1}{\epsilon_0}\sum_{i=1}^{3}\int_{C_i} q_i(\mathbf{r}')\ln|\mathbf{r}-\mathbf{r}'|dl' = V(\mathbf{r}) = V_0, \quad \mathbf{r} \in \bigcup_{i=1}^{3} C_t \tag{2}$$

In the present work (2) has been numerically solved by a 2-D electrostatic MoM code [10], based on circular harmonics expansion, which computes all quantities in a few seconds.

2.1.1 Antenna mode: In the antenna mode scheme (Fig. 2*a*), the structure is sourced by three equal voltage generators $V_A^{(1)} = V_A^{(2)} = V_A^{(3)} = V_A$ and the currents over conductors have the same direction (according to the first column of the matrix in (1)). The three conductors are equivalent to a single conductor with discontinuous equivalent radius. Denoting with Y_A the input admittance of this dipole, where a *δ-gap* is inserted in correspondence to the taverse plane through port 1 and port 2, then

$$I_A = V_A Y_A \tag{3}$$

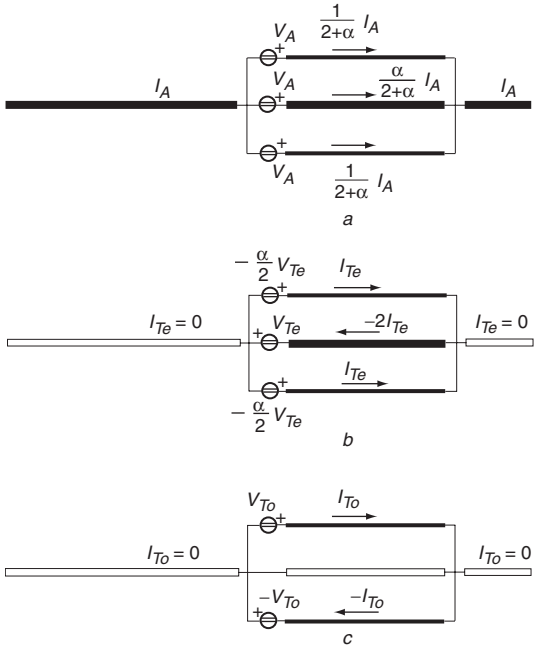

Fig. 2 *Decomposition of the three-conductor antenna*
a Antenna mode scheme and two coupled transmission line modes
b Even excitations
c Odd excitations

2.1.2 Transmission line even mode: In this mode (Fig. 2*b*), the sum of transmission line currents is zero and there is no current on the main conductor: the structure does not radiate. Denoting with V_{Te} the voltage at port 3, the voltage drop at the other ports is

$$V_{Te}^{(2)} = V_{Te}^{(1)} = -\frac{\alpha}{2}V_{Te}$$

Owing to the symmetry, the three-conductor transmission line can be viewed as a pair of coupled transmission lines under even-mode excitation with current I_{Te} and voltage generators

$$V_{Te}^{(1)} - V_{Te} = V_{Te}^{(2)} - V_{Te} = -(\tfrac{\alpha}{2}+1)V_{Te}$$

for which we have

$$I_{Te} = -\tfrac{\alpha+2}{2}Y_{stub,e}V_{Te} \tag{4}$$

where $Y_{stub,e}$ is the input admittance of a circuit comprising a stub of length ℓ and two short conductors, of length s and radius r, connecting the towel bar to the aircraft body. Each of them is modelled [11] as an inductor of value

$$L_{end} = \frac{\mu_0}{2\pi}s[\ln(2s/r) - 1]$$

2.1.3 Transmission line odd mode: Also, in this mode (Fig. 2*c*) the structure does not radiate. The current on the conductor 3 (I_{To}) is zero, the currents on conductor 1 and 2 are of opposite directions and therefore $V_{To}^{(1)} = -V_{To}^{(2)} = V_{To}$ and $V_{To}^{(3)} = 0$. Coupled transmission line theory gives the input current in terms of input admittance $Y_{stub,o}$ of the odd-mode excited stub circuit.

$$I_{To} = Y_{stub,o}V_{To} \tag{5}$$

Even and odd modal characteristic impedances η_e and η_o can be easily computed by the same MoM code used to solve (2).

By taking into account the boundary condition ($V_2 = 0$ and $V_3 = 0$) required to calculate the admittance matrix, it is easily shown that, by superposition of the three schemes, the following expressions can be obtained:

$$\begin{aligned} Y_{11} = Y_{22} &= \frac{Y_A}{(\alpha+2)^2} + \frac{1}{2}Y_{stub,e} + \frac{1}{2}Y_{stub,o} \\ Y_{12} = Y_{21} &= \frac{Y_A}{(\alpha+2)^2} + \frac{1}{2}Y_{stub,e} - \frac{1}{2}Y_{stub,o} \end{aligned} \tag{6}$$

For these relationships, the equivalent T-circuit scheme (Fig. 3*a*), rather than a π-scheme, gives a simple representation where the contributions of the three modes are well separated. It is worth noticing that, in the case of a single towel-bar antenna, this circuit reduces to a corrected version of the Γ-match circuit presented in [8], where the dipole admittance is erroneously multiplied by a factor of two.

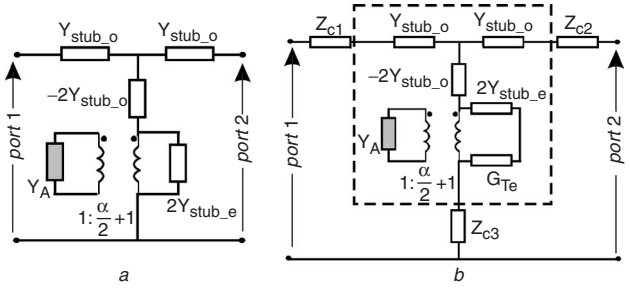

Fig. 3 *Equivalent circuits*
a Basic equivalent T-network for the two towel bar antenna system on a locally cylindrical body
b Enhanced version, incorporating transmission line radiation (within box) and conductor losses
Y_A denotes the input admittance of the antenna mode while $Y_{stub,e}$ and $Y_{stub,o}$ characterise the transmission line modes

A more accurate network model, accounting for radiation from transmission line currents and particularly useful at low frequencies, can be derived in the hypothesis of a small angle between the loops ($\phi_0 \ll 90°$). Under this assumption, the structure with even-mode excitation roughly radiates as two strongly coupled vertical half loops over a perfect ground plane having a common input port and radiation conductance $G_{Te} = (40k_0^4 s^2 \ell^2)^{-1}$ for $\ell \ll \lambda$. Since the odd-mode currents on the loop are of opposite phase, the radiation from odd-mode currents is neglected and the equivalent circuit is modified as shown in the boxed portion of Fig. 3*b*.

2.2 Effect of conductor losses

The influence of conductor losses can be introduced into the model by adding lumped impedances to the equivalent circuit. These impedances are estimated under the hypothesis that the current on the loop is almost constant and that the influence of the surrounding objects may be neglected. This approximation holds only at low frequencies. At higher frequencies, the radiation resistance dominates over the loss resistance.

Denoting with Z_s the surface impedance of the wire, the internal impedances of loop conductors can be computed, neglecting the proximity effect owing to a large cylinder, as

$$Z_{c1} = Z_{c2} = \frac{\ell}{2\pi r} Z_s$$

Losses on the cylinder are taken into account by a simplified planar static model [12] and the corresponding loss impedance can be then modelled by

$$Z_{c3} = (Z_s/\pi)\cosh^{-1}\frac{\ell}{2r}$$

The resulting equivalent network is shown in Fig. 3*b*.

3 Combined approach

The combined FDTD–MTL method is now described with reference to a real structure. The antenna mode input admittance Y_A is computed for a coarse-grid FDTD model of the aircraft without the loops. This model will include only the most relevant geometrical details and neglect loop antenna conductors since they do not significantly affect the equivalent radius. To calculate the input admittance, a delta gap excitation is used to source the fuselage on to the cross-section corresponding to the loop ports. Time to frequency Fourier transform of current and voltage at the feed point permits calculation of the antenna mode input admittance within the whole bandwidth of the excitation signal.

The MTL parameters α, η_e, η_o are calculated for the real cross-section of the fuselage by a 2D-static MOM. The resulting network parameters (self and mutual input impedances) of the whole structure are therefore quickly computed by (6). It is worth noticing that a change in the loop length only requires a new circuit analysis, while a modification in the angle ϕ_0 requires recalculation of the MTL parameters. A new electromagnetic FDTD analysis is needed only for different longitudinal position of the loops.

Besides the electromagnetic data reusability, this decomposition approach has the non-negligible benefit to greatly speed up the FDTD computation since the high-Q loops are not included in the simulation.

4 Validations and examples

Two examples are reported involving a scaled model of an aircraft fuselage, which has also been built and measured, and a full-scale simplified model of a transportation aircraft, including wings and stabilisers. The code BEST [13] has been used for all FDTD simulations.

4.1 Scaled model of an aircraft fuselage

For measurement feasibility, a scaled model (1:35) of an aircraft fuselage (Fig. 4) has been considered within the

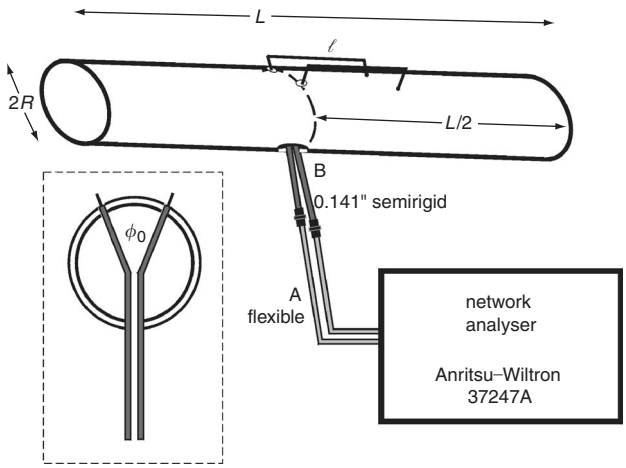

Fig. 4 *Experimental set-up*
Antenna ports are positioned in the middle cross-section. $L = 686$ mm, $R = 50$ mm, $\ell = 103$ mm, $\phi_0 = 45°$, $s = 7$ mm, loop wire diameter 0.72 mm

range 40–1000 MHz. Measurements are compared with the solution obtained by means of the novel method and more conventional simulation tools. To minimise the interaction with the measurement equipment (cables), towel bar antennas have been placed such that their input ports are connected to the central cross-section of the tube; in this way, only fuselage currents with longitudinal symmetry, with respect to the central cross-section, are excited. The structure, which is supported by a dielectric tripod, consists of a copper tube ($\sigma = 5.8\ 10^7$ S/m) with closed extremities. To preserve the antenna symmetry, the feeding cables are disposed along a radial direction of the tube, on the symmetry plane orthogonal to the tube axis.

To apply the new method, an FDTD computation of the cylinder without loops has been performed on a coarse cartesian grid ($\Delta x = \Delta y = 1.657$ cm, $\Delta z = 2.213$ cm) for a global domain of $36 \times 36 \times 61 \cong 79\ 10^3$ voxels. The voltage time dependence for the δ-gap excitation has been chosen as a Gaussian pulse with -20 dB bandwidth of 0–1 GHz. The parameters of the network model of the towel bar antennas, as computed by the static two-dimensional MoM code, are $\alpha = 26.01$, $\eta_e = 226.7\,\Omega$, $\eta_o = 219.7\,\Omega$.

To provide reference solutions, MoM and FDTD simulations of the full detailed structure have been carried out. A wire-mesh model of the tube with loops has been used for MoM (NEC2D solver) analysis while a finer discretisation ($\Delta x = \Delta y = \Delta z = 3.57$ mm, for overall $76 \times 70 \times 231 \cong 1.2\ 10^6$ voxels) has been required by FDTD to properly accommodate the antenna details. In the FDTD model, the ohmic losses of the loops and of the tube are approximately taken into account in the post-processing by adding to the FDTD computed Z_{11} and Z_{12} the previously introduced loss impedances Z_{c1}, Z_{c2} and Z_{c3}.

The measured and simulated Z-parameters of the antenna systems are presented in Figs. 5 and 6. In spite of some artefacts, there is substantial agreement between the different sets of data from low frequencies up to the loop antiresonance, occurring around 650 MHz, although the fullwave finer-grid FDTD analysis calculates smaller self-resistance at the lower bound of the band ($f < 150$ MHz). The first longitudinal resonance of the copper tube, occurring at about 200 MHz, is clearly visible mainly in the mutual resistance and excellent agreement is observed among all the data sets. Beyond the loop antiresonance, a reduced agreement is apparent because of the excitation of tube currents with significant transversal (circumferential) components, which are not taken into account by the proposed model. For the same reason, the feeding coaxial cables begin to interact with the structure and the measurements are less accurate.

The computation times required by the different methods used in the numerical simulations are reported in Table 1. As expected, the new method is about two orders of magnitude faster and consumes less memory than fullwave solvers. The great difference in the computation time, only partially due to the larger grid of the fullwave FDTD, is related to the high oscillating regime of the fullwave analysis imposed by the high Q-factor of the loop antennas.

Table 1: Computer resources for the numerical solution of the loops and tube problem

Method	Domain size	Run time
Full-detail MOM	1976 segments	12 min/frequency
Full-detail FDTD	$1.2\ 10^6$ voxels	604.5 min
New method	$79\ 10^4$ voxels	7 min (coarse FDTD) +0.2 min (2D-MoM)

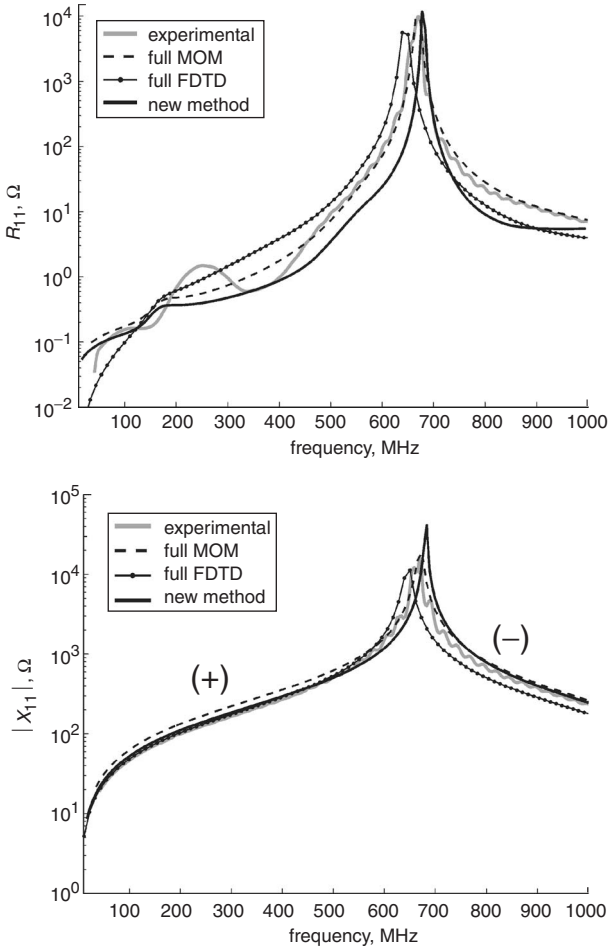

Fig. 5 *Self impedance of the towel bar antenna system on the copper tube obtained from measurements, by means of fullwave models of the whole structure including the loops and by the new method*

The reactance is expressed by absolute value to better appreciate the large dynamic. Signs '+' and '−' indicate the inductive and capacitive regions, respectively.

4.2 Full-scale realistic model of a transportation aircraft

The new method will be now applied, within the 0–35 MHz band, to a more detailed full-scale model of an aircraft (Fig. 7) including the wings and both the horizontal and vertical stabilisers. Conductor losses are included, as described in Section 2.2, assuming a conductivity $\sigma = 3.6\ 10^7$ S/m which is typical of some aluminium alloys. Towel bar antennas are placed as shown in the aforementioned Figure and each one of them is fed at the end towards the prow.

This geometry has been first simulated by a fine-grid FDTD, including the antennas, to provide a reference solution for the FDTD–MTL combined method involving a coarse-grid FDTD. In the former simulation, a nonuniform grid has been used with voxel sizes $0.1 \le \Delta x$, Δy, $\Delta z \le 1$ m for an overall simulation domain of $1.2 \cdot 10^6$ voxels. The coarse-grid simulation, used in the FDTD–MTL method, employs a uniform grid ($\Delta x = \Delta y = 0.58$ m, $\Delta z = 0.76$ m) of $224\ 10^3$ voxels. The aircraft admittance Y_A is shown in Fig. 7, where the first and second fuselage resonances (occurring around 4.5 MHz and 7.5 MHz) are clearly visible.

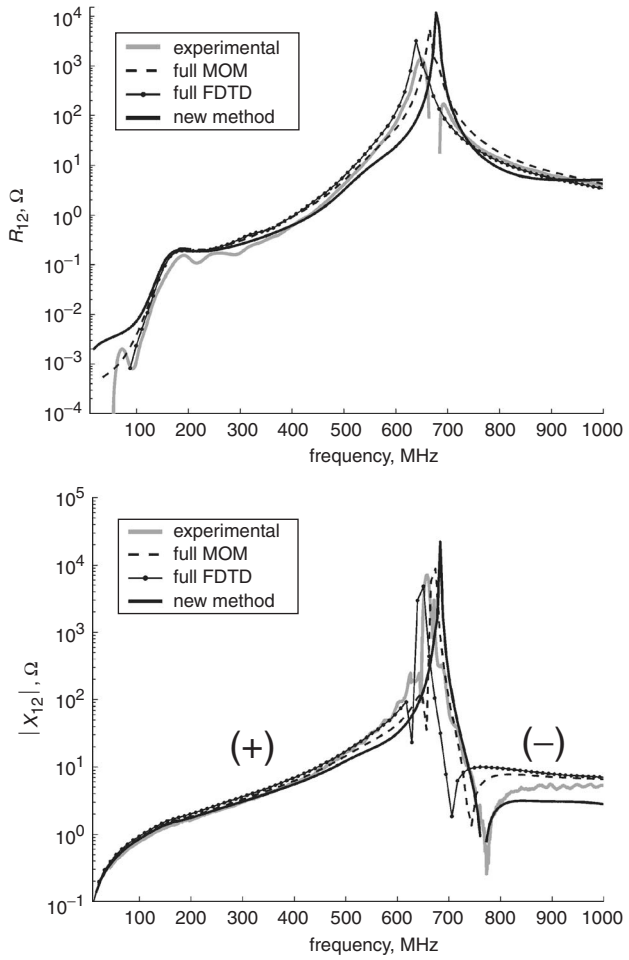

Fig. 6 *Mutual impedance of the towel bar antenna system on the copper tube obtained from measurements, by means of fullwave models of the whole structure including the loops and by the new method*

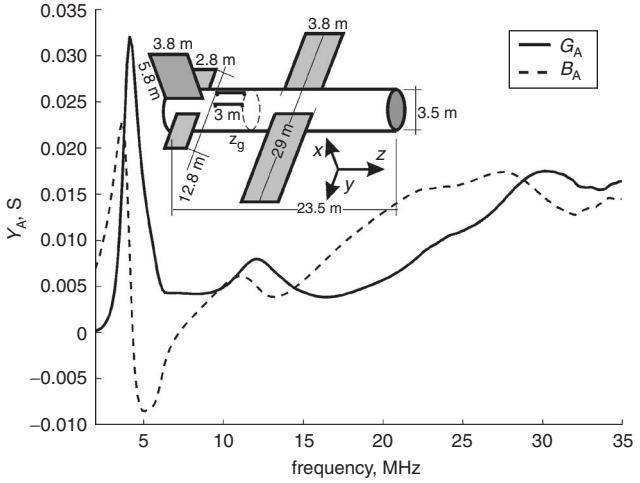

Fig. 7 *Realistic model of a full-scale transportation aircraft; gap input admittance of the aircraft loop-free model computed by a coarse-grid FDTD*

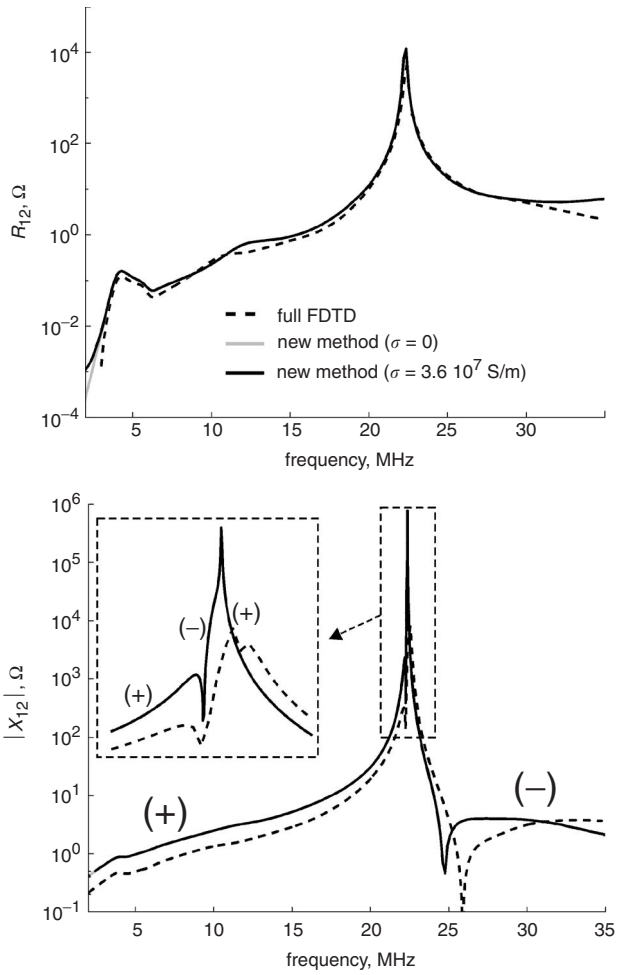

Fig. 8 *Mutual impedance for the full-scale aircraft model when the angular spacing of the towel bar antennas is 45°*
Solutions have been obtained by a fully detailed FDTD model, including the antennas, and the proposed method with or without loop ohmic losses. Grey and black lines are indistinguishable in the reactance plot.

The comparison over the mutual impedance for an angular spacing $\phi_0 = 45^\circ$ is shown in Fig. 8. An excellent agreement can be appreciated within the entire frequency range. It is interesting to note that, as expected, the circuit model including the conductor losses shows a higher impedance at low frequencies.

The computation times have been 5.5 h for the fully detailed FDTD and 15 min for the proposed combined method.

To discuss the flexibility of the new method in parametric analysis, the impedance matrix has been computed for different values of antenna angular spacing and length. The sweep over angular spacing ϕ_0 requires only the solution of the aforementioned 2-D static problem to compute α, η_e and η_o, while new electromagnetic runs are avoided. Fig. 9 shows an example, computed in a few seconds, where ϕ_0 has been swept from 2° to 180°. The mutual reactance is the most sensitive parameter to angular spacing variations and the mutualantenna coupling decreases at both low and high frequencies as ϕ_0 increases. It has also been verified that, when the angular spacing is larger than 15°, the other impedance parameters Z_{11} and R_{12} are almost insensitive to the angular position of the antennas.

The analysis of the antenna performances against loop length for a fixed ϕ_0, requires the only change of the odd-mode and even-mode input admittances of the stubs. As an example, Fig. 10 shows antenna input impedances for $2\,\text{m} \leq \ell \leq 4\,\text{m}$; the most evident effects of the loop length are both the shift of the loops antiresonances and a reduction in the antenna coupling as ℓ decreases.

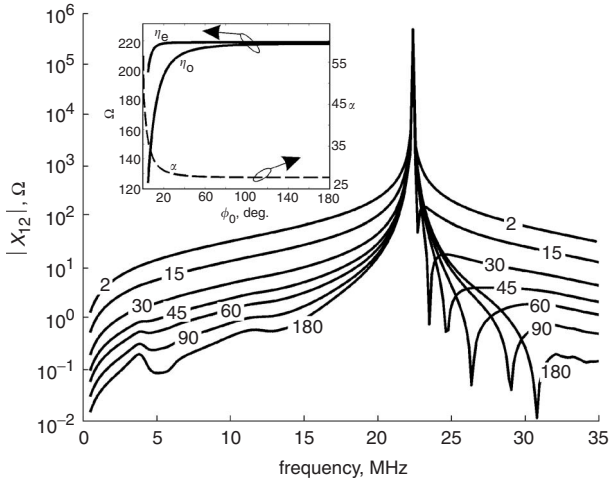

Fig. 9 *Mutual reactance against frequency for different values of the loops angular spacing (labelled in degrees)*
Within the inset, the plots of the current division factor α and of the even mode and odd-mode characteristic impedances against ϕ_0.

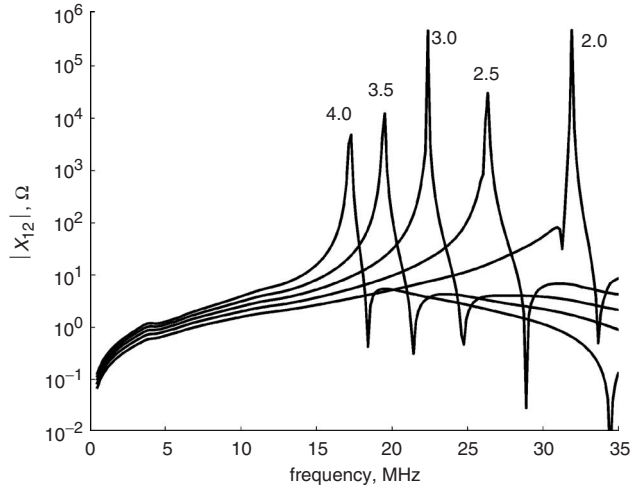

Fig. 10 *Mutual reactance for several antenna lengths (labelled in m) for a fixed angular spacing $\phi_0 = 45^\circ$*

5 Conclusions

The proposed combined method, based on FDTD and a generalisation of the Γ-match concept, permits an almost instantaneous computation of self and mutual input impedance between aircraft towel bar antennas by means of a 2-D electrostatic analysis plus a fast numerical simulation of the aircraft without antennas. Application to fully and locally cylindrical structures has shown results in good agreement with reference solutions (better than those proposed by other authors in the past).

The method can be extended to the analysis of more complex antennas with loops of unequal lengths and the electromagnetic formulation can also be improved for fast prediction of the radiation diagrams.

6 Acknowledgments

This work has been partially funded by MARCONI-SELENIA, Finmeccanica Group. The authors wish to thank K. Barrie for support, and M. Proia and R. Perelli, of the above company, for suggestions and valuable discussions.

7 References

1 Cox, J.W.R.: 'Corroboration of a moment-method calculation of the maximum mutual coupling between two HF antennas mounted on a helicopter', *IEE Proc. Microw. Antennas Propag-H*, 1995, **140**, (2), pp. 113–120
2 Helbing, S., Cryan, M., Alimenti, F., Mezzanotte, P., Rosselli, L., and Sorrentino, R.: 'Design and verification of a novel crossed dipole structure for quasi-optical frequency doublers', *IEEE Microw. Guided Wave Lett.*, 2000, **10**, (3), pp. 105–107
3 King, R.W., and Harrison, C.W.: 'Antennas and waves' (MIT Press, Cambridge, 1969)
4 Geogakopoulos, S.V., Balanis, C.A., and Birtcher, C.R.: 'Coupling between transmission line antennas: analytic solution, FDTD, and measurements', *IEEE Trans. Antennas Propag.*, 1999, **47**, (6), pp. 978–985
5 Marrocco, G., and Tognolatti, P.: 'A combined fullwave/network model for analysis and design of airborne HF loop antennas'. 9th Int. Conf. on HF radio systems and techniques, Bath, UK, June 2003, pp. 216–221
6 Taflove, A.: 'Computational electrodynamics: the finite-difference time-domain method' (Artech House, Norwood, MA, USA, 1995)
7 Uda, S., and Mushiake, Y.: 'Yagi-Uda antenna' (Sasaki Printing and Publishing Co., Japan, 1954)
8 Tolles, H.T.: 'How to design gamma-matching networks', *Ham Radio*, 1973, pp. 46–55
9 Lampe, R.W.: 'Design formulas for an asymmetric coplanar strip folded dipole', *IEEE Trans. Antennas Propag.*, 1985, **33**, (9), pp. 1028–1031
10 Paul, C.R.: 'Analysis of multiconductor transmission lines' (Wiley Inc., England, 1994)
11 Terman, F.E.: 'Radio engineers' handbook' (McGraw–Hill, 1943)
12 Smythe, W.R.: 'Static and dynamic electricity' (Taylor & Francis, 1989, 3rd edn)
13 Marrocco, G., and Bardati, F.: 'BEST: a finite-difference solver for time electromagnetics', *Simul. Prac. Theory*, 1999, **7**, (3), pp. 279–293